ChemPlusChem

Research Article
doi.org/10.1002/cplu.202400169

Chemistry Europe
European Chemical Societies Publishing

www.chempluschem.org

Bifunctional Metal-Organic Nanoballs Featuring Lewis Acidic and Basic Sites as a New Platform for One-Pot Tandem Catalysis

Gaurav Verma[+],[a] Sanjay Kumar,[b] Elliott R. Slaughter,[c] Harsh Vardhan,[d] Thamraa M. Alshahrani,[e] Zheng Niu,[f] Wen-Yang Gao,[g] Lukasz Wojtas,[h] Yu-Sheng Chen,[i] and Shengqian Ma*[a]

The design and synthesis of polyhedra using coordination-driven self-assembly has been an intriguing research area for synthetic chemists. Metal-organic polyhedra are a class of intricate molecular architectures that have garnered significant attention in the literature due to their diverse structures and potential applications. Hereby, we report **Cu-MOP**, a bifunctional metal-organic cuboctahedra built using 2,6-dimethylpyridine-3,5-dicarboxylic acid and copper acetate at room temperature. The presence of both Lewis basic pyridine groups and Lewis acidic copper sites imparts catalytic activity to Cu-MOP for the tandem one-pot deacetalization-Knoevenagel/Henry reactions. The effect of solvent system and time duration on the yields of the reactions was studied, and the results illustrate the promising potential of these metal-organic cuboctahedra, also known as nanoballs for applications in catalysis.

[a] *Dr. G. Verma,[+] Prof. S. Ma*
Department of Chemistry
University of North Texas
1508 W Mulberry St., Denton, Texas 76201, USA
E-mail: Shengqian.Ma@unt.edu

[b] *Dr. S. Kumar*
Department of Chemistry
Multani Mal Modi College
Modi College, Lower Mall, Patiala, Punjab 147001, India

[c] *E. R. Slaughter*
Texas Academy of Mathematics and Sciences
University of North Texas
1508 W Mulberry St., Denton, Texas 76201, USA

[d] *Dr. H. Vardhan*
Department of Chemical and Biomolecular Engineering
Rice University
6100 Main St., Houston, Texas 77005-1827, USA

[e] *Prof. T. M. Alshahrani*
Department of Physics, College of Science
Princess Nourahbint Abdulrahman University
Riyadh11564, SaudiArabia

[f] *Dr. Z. Niu*
College of Chemistry, Chemical Engineering and Materials Science
Soochow University
Suzhou, Jiangsu 215123, People's Republic of China

[g] *Dr. W.-Y. Gao*
Chemistry & Biochemistry Department
Ohio University
Athens, Ohio 45701, USA

[h] *Dr. L. Wojtas*
Department of Chemistry
University of South Florida
4202 E. Fowler Ave, Tampa, Florida 33620, USA

[i] *Dr. Y.-S. Chen*
ChemMatCARS, Center for Advanced Radiation Sources
The University of Chicago
9700 South Cass Avenue, Argonne, Illinois 60439, USA

[+] *The submission is a part of thesis of the first author Gaurav Verma.*

Supporting information for this article is available on the WWW under https://doi.org/10.1002/cplu.202400169

Introduction

Supramolecular chemistry is a dynamic and interdisciplinary field at the intersection of chemistry, materials science, and nanotechnology that facilitates the creation of intriguing architectures through both covalent and non-covalent interactions, enabling chemists to design and create functional materials with unique properties and applications.[1] Coordination-driven self-assembly presents additional possibilities for generating structures with predetermined shape, size, and symmetry.[2] Employing this bottom-up methodology has enabled the design and synthesis of various nanoscopic metal-organic materials (MOMs), encompassing coordination networks, metal-organic frameworks (MOFs), and metal-organic polyhedra (MOPs).[3]

Nanoballs, the molecular versions of faceted polyhedra, stand out as distinctive and fascinating structures within the realm of MOPs. Typically comprised of metal(II) paddlewheels interconnected at a 120° angle by angular bifunctional ligands like benzene-1,3-dicarboxylate (bdc) or its derivatives, nanoballs exhibit discrete architectures.[4] The typical structure is $[M_2(R\text{-}bdc)_2(L)_2]_{12}$, where M(II) can be Cu(II), Cr(II), Mo(II), Ru(II), Rh(II), or heterobimetallic species. Here, R represents 5-OH, 5-$OC_{12}H_{25}$, 5-t-Bu, 5-SO_3^-, 5-NH_2, or other similar variants, while L denotes a solvent axially coordinated or a mixture of solvents like H_2O, EtOH, DMF, and DMSO.[5–7] Twelve pairs of dinuclear M(II)-M(II) paddlewheel units are linked together by 24 R-bdc units, forming a discrete cuboctahedral architecture featuring eight triangular and six square openings that lead into an inner cavity of 1.5–1.9 nm in size.[6] Cuboctahedral structures derived from m-bdc measure approximately 2.5 nanometers in size and exhibit variability dependent on the size of their substituents.[4e]

Nanoballs hold immense promise for a range of applications, including guest inclusion, adsorption and separation,

drug delivery, sensing, and catalysis, owing to their precisely defined cavities and permanent porosity.[8] Moreover, the characteristics of these distinct frameworks can be altered through (a) the design of the ligand backbone[4e] and (b) post-synthetic functionalization of the peripheral ligand and metal paddlewheel units,[6,7a,9a–b] leading to the emergence of intriguing features. These frameworks have been employed as molecular building blocks (MBBs) in the assembly of more complex materials such as MOFs,[4a,9b–h] exfoliated into MOF nanosheets,[9i] integrated into nanoball-polymer composites (such as polyurethanes and PMMA) and hybrid membranes,[10] and solubilized in both polar and non-polar solvents.[10b,f,11] Encapsulating nanoballs within the voids of other porous materials like mesoporous silica and MOFs,[12] along with shielding their outer periphery,[6,13a] has demonstrated the ability to bolster the stability of these structures. This approach prevents aggregation and collapse upon solvent removal.

Indeed, nanoballs have been extensively employed in gas adsorption and separation,[5a,10a,f,12c,13a–b] environmental remediation,[13c] and as artificial ion channels for biomedical applications.[4c, 9b,13d–e] However, MOPs are still relatively under-explored compared to their MOF counterparts,[8b] warranting significant attention due to their aforementioned capabilities. The design and exhibition of divergent catalytic sites, notably acidic and basic sites, within a single system have emerged as a compelling aspect of MOF catalysts.[14] Typically, multiple catalytic sites are integrated into the robust architectures to ensure their compatibility. However, the creation of a catalytic system featuring multiple functionalities within a nanoball architecture for sequential synthesis remains unparalleled. Nanoballs hold promise as highly efficient catalysts due to their confined and precisely defined internal cavities, active metal sites, high symmetry, and diverse chemical and physical properties. Moreover, unlike MOFs and other heterogeneous catalysts, nanoballs can be solubilized thus affording the features of both homogeneous and heterogeneous catalysts within one system.[11b]

While the method employed to produce nanoballs through the self-assembly of bdc derivatives might seem straightforward, it does not always exclusively yield these distinct architectures. Various outcomes can result from the process, including the formation of one-, two-, or three-dimensional coordination networks.[4c,8b–c,10b,15] The parameters affecting the self-assembly process encompass pH, concentration, temperature, solvent, as well as the steric and electronic effects of the substituents.[6,10b,15c,16] Thermodynamic principles tend to support structures that have minimal or no empty spaces, and numerous metastable products can emerge if the reaction is governed by kinetic control. Fundamental design guidelines prioritize upholding both the structural and functional compatibility among the building blocks, while also ensuring that interaction sites are appropriately positioned relative to each other. This guarantees the feasibility of constructing the desired discrete structure, and then suitable reaction conditions must be established.[10b,11b] Iterative experimentation is crucial for determining the suitable reaction conditions. Leveraging insights from existing literature and employing intuitive reasoning can streamline the trial-and-error process, ultimately reducing the number of attempts and facilitating the achievement of the desired structure.[11b]

In this communication, we present a bifunctional discrete metal-organic cuboctahedron, **Cu-MOP**, synthesized from copper acetate and 2,6-dimethylpyridine-3,5-dicarboxylic acid, exhibiting Lewis acidic and basic functionalities. **Cu-MOP** is efficiently synthesized in high yield and serves as an effective catalyst in the deacetylation-Knoevenagel and deacetylation-Henry reactions.

Results and Discussion

Crystal Structure Description

The thermodynamic stability of nanoballs over dinuclear copper(II) carboxylates in organic solvents is well-documented.[11b] However, their stability notably decreases in aqueous solutions. Additionally, solvents like DMF, DMSO, and methanol enhance the kinetic stability of nanoballs with interconnected copper(II) paddlewheels compared to more labile dinuclear copper(II) complexes like copper(II) acetate. Furthermore, the self-assembly of discrete architectures is significantly influenced by factors such as concentration and the metal-to-ligand ratio, which are of utmost importance as established by the groups of Larsen and Volmer.[11b,16] In light of this understanding, we aimed to synthesize nanoballs constructed from copper(II) acetate and 2,6-dimethylpyridine-3,5-dicarboxylate (**L**), a ligand characterized by Lewis basic pyridyl nitrogen atoms. By dissolving equal amounts of the two components in DMF and subsequently subjecting them to gravimetric diffusion with methanol at room temperature, we successfully obtained the discrete nanoball architecture. (Figure 1). Over a span of 12 hours, blue rod-shaped crystals were obtained. The as-synthesized sample was subject to purification via multiple washes with a 1:4 mixture of DMF and CH_3OH,

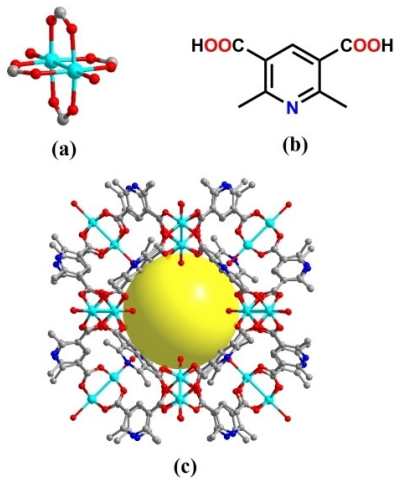

Figure 1. The (a) copper paddlewheel SBU, (b) 2,6-dimethylpyridine-3,5-dicarboxylate linker (**L**), and (c) resulting $Cu_{24}L_{24}$ polyhedral cage.

followed by CH_3OH alone, resulting in the isolation of pure **Cu-MOP** with 73% yield.

Cu-MOP crystallized in a hexagonal *P6₃/mcm* space group. Its structure is composed of $M_{24}L_{24}$ cuboctahedra, wherein the 12 dicopper units serve as vertices and the ligands from the edges. As anticipated, the structure resembles that of other discrete nanoballs documented in the literature, built from Cu(II) and bdc derivatives.[4,5] The average Cu–O bond distance for carboxylate is 1.90(2) Å, while for Cu–O (water) it is 2.07(2) Å. The average Cu–Cu distance is 2.63(5) Å, consistent with previously reported dicopper paddlewheels. Each copper(II) paddlewheel unit features two solvent molecules modeled as water at the axial positions. Pyridyl nitrogen atoms adorn the structure's periphery, with the two methyl groups at the 2,6-positions forming a C–N–C angle of approximately 169°.

The configuration of these two methyl groups is quite important, as efforts to achieve the nanoball architecture for pyridine-3,5-dicarboxylate consistently resulted in the formation of the 3D MOF structure, where the pyridyl nitrogen atoms bind to the copper(II) atoms to construct the network..[17] Furthermore, subjecting Cu(II) and **L** to hydrothermal reaction at 80 °C produces a mononuclear complex, whereas conducting the reaction at 140 °C results in a 2D network structure featuring a 32-membered macrometallacycle characterized by a parallelogram-like (4,4) topology.[18] Hence, employing DMF/MeOH as the organic solvent at ambient conditions yielded the kinetically stabilized self-assembled discrete nanoball architecture.

Powder X-ray diffraction (PXRD) measurements were conducted to determine the bulk phase purity of the compound. The results revealed a good agreement between the calculated and observed PXRD patterns (Figure 2a). Additionally, the framework exhibited thermal stability up to 220 °C (Figure S2) following the initial removal of solvent molecules as indicated by thermogravimetric analysis (TGA).

Surface Area and Porosity Measurements

Gas adsorption measurements were employed to investigate the permanent porosity of **Cu-MOP**. Traditional activation methods were not applicable to this material, as it exhibited no porosity after activation in methanol followed by evacuation for 12 hours at 60 °C. Consequently, activation was achieved through supercritical CO_2 drying after solvent exchange using methanol, followed by heating the exchanged material at 60 °C under dynamic vacuum for 10 hours. Surface area measurements were performed using CO_2 at −78 °C. The Langmuir surface area depicted in Figure 2b was found to be 260 m^2/g, with a corresponding pore volume of 0.18 cm^3/g. According to the DFT model, the pore size was determined to be 11.79 Å, consistent with observations from the crystal structure. At 1 bar, the CO_2 uptake capacity was 43 and 30 cm^3/g at 0 and 25 °C, respectively (Figure 3).

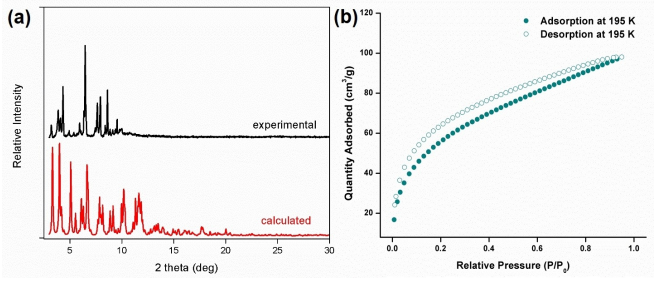

Figure 2. Characterization of the Cu-MOP: (a) Comparison of the experimental (black) and calculated (red) PXRD patterns, and (b) Langmuir surface area measurements using CO_2 adsorption-desorption isotherms at 195 K.

Catalytic Activity for Tandem One-Pot Synthesis

In the realm of sustainable chemistry, multicomponent reactions garner particular interest due to their high efficiency, atom economy, and minimal waste generation.[14] The synergistic effects further enhance the prominence of multifunctional catalysts, thus attracting considerable attention. Given that Cu-MOP encompasses Lewis acidic sites represented by copper(II) paddlewheels, which can be activated following solvent removal, along with Lewis basic sites on the ligand backbone in the form of pyridyl nitrogen atoms, we aimed to employ it as a catalyst in tandem reactions.

We first utilized **Cu-MOP** as an effective catalyst for the one-pot deacetylation-Knoevenagel condensation reaction. Deacetylation typically requires an acid catalyst, while the Knoevenagel condensation reaction is facilitated by a base (Scheme 1), both well-documented in the literature.[19] **Cu-MOP** exhibits remarkable catalytic activity in this reaction, yielding benzylidene-

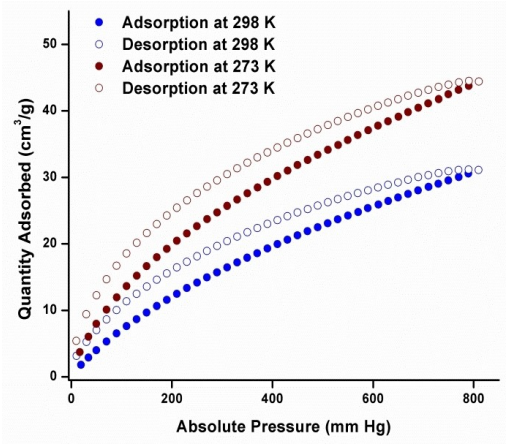

Figure 3. CO_2 adsorption-desorption isotherms at 273 K and 298 K.

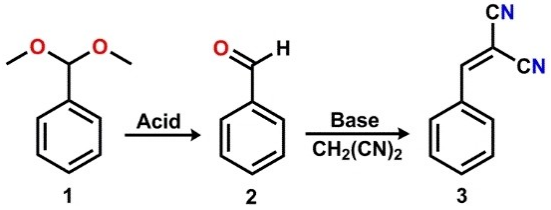

Scheme 1. The one-pot deacetalization-Knoevenagel condensation reaction.

malononitrile through sequential deacetylation and Knoevenagel condensation reactions. The yield of the product was 92% using **Cu-MOP** as the catalyst in DMSO for 20 h. Control experiments without the catalyst yielded the product in negligible amounts. To establish the effects of the Lewis basic pyridinic nitrogen atoms, c-MOP[4b] containing only the bdc ligand and a physical mixture of the two reagents were also utilized as catalysts. The physical mixture was not heated due to the possibility of forming coordination architectures in DMSO. Table 1 shows that these reactions were not able to achieve the high yield obtained using Cu-MOP, indicating the synergistic effect between both types of active sites in the same catalyst architecture.

Various solvents such as methanol, toluene, dioxane, tetrahydrofuran (THF), acetonitrile and dimethylsulfoxide (DMSO) at different temperatures were explored (Figure 4 and Table S4), and the highest yields were observed using DMSO as the solvent (62% yield, 50 °C, 12 h). The effect of time duration and temperature on the yield of the reaction in DMSO was also evaluated, with the optimal results achieved using DMSO at 70 °C for 20 hours (92%). The enhanced yield observed with DMSO can be attributed to its higher polarity, which stabilizes the malononitrile anion intermediate.[20]

During the 12-hour period (Table 2), the yields are lower compared to MOF counterparts such as Cu-PCN-126 (99%) and PCN-124 (100%),[21] but similar to HNUST-6 and HNUST-8,[22] which achieve 100% yields over a 48-hour period. Expanding the substrate scope, we utilized 4-Methoxybenzaldehyde dimethylacetal and attained a yield of 98% owing to increased ring electron density, facilitating faster aldehyde formation from the acetal. However, for 4-Bromobenzaldehyde diethyl acetal, minimal product was observed due to challenges in converting the aldehyde to the acetal.

The recyclability of the catalyst was also evaluated and it could be used for at least four cycles without much significant loss in activity (Figure 5). The material showed good stability over the catalytic runs as evident from the PXRD patterns (Figure S4), however a slight loss in crystallinity of the **Cu-MOP** after the fourth cycle was observed.

Based on the existing literature,[23] a potential reaction mechanism for the one-pot deacetalization-Knoevenagel reaction catalyzed by the bifunctional **Cu-MOP** catalyst can be proposed. Initially, unsaturated Lewis acidic Cu sites catalyze the hydrolysis of benzaldehyde dimethylacetal to benzaldehyde. These Lewis acid sites then further interact with the carbonyl oxygen of benzaldehyde, activating it. Basic pyridyl sites on the framework deprotonate the methylene group of malononitrile, generating the malononitrile carbanion. Subsequently, the activated aldehyde carbonyl undergoes nucleophilic attack by the malononitrile carbanion, yielding the desired benzylidenemalononitrile through the loss of a water molecule with the regeneration of the catalyst for the next run. To unravel the detailed catalytic mechanism and gain deeper insights into the interactions of the substrates with the catalytic Lewis acidic/basic sites, we will carry out further theoretical studies in the future work.

To further demonstrate the generality of **Cu-MOP** for tandem reactions and expand its scope, we utilized it in the catalytic one-pot deacetalization-Henry reaction between benzaldehyde dimethylacetal and nitromethane as shown in Scheme 2. Remarkably, the material showed good catalytic activity for this reaction as well, generating high yields for the resultant β-nitrostyrene (91%, DMSO, 24 h) as shown in Table 3.

Table 1. The yield of the product **3** using different catalysts.[a]

Catalyst	Yield of **3** (%)
Cu-MOP	92
c-MOP[4b]	35
No catalyst	Trace
Physical mixture[b]	42

[a] Reaction conditions: 2 mmol of each substrate in solvent (2 mL) and the catalyst (50 mg) in a 10 mL reaction tube at a 70 °C under a N_2 atmosphere for 20 h. [b] The reaction was carried out at room temperature.

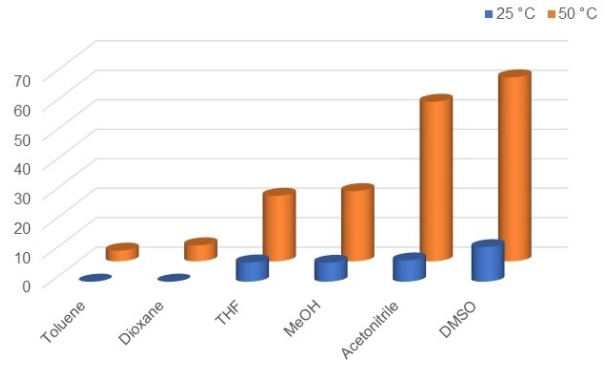

Figure 4. Effect of variation of temperature and solvent on yield of the product.

Table 2. Optimization of the time duration in DMSO at 70 °C.

Time (h)	Yield (%)
4	30
12	75
20	92

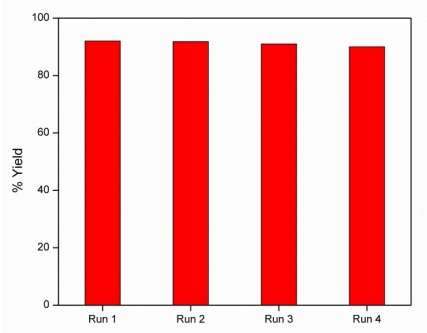

Figure 5. The recyclability tests demonstrating negligible loss in the catalytic activity over four cycles.

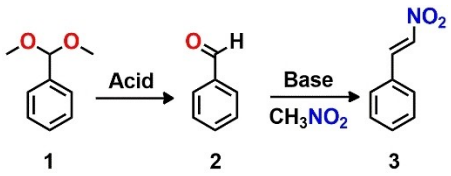

Scheme 2. The one-pot deacetalization-Henry reaction.

Table 3. The yield of the product **3** using different catalysts.[a]

Catalyst	Solvent	Yield of **3** (%)
Cu-MOP	DMSO	91
No catalyst	DMSO	Trace

[a] Reaction conditions: 2 mmol of each substrate in solvent (2 mL) and the catalyst (50 mg) in a 10 mL reaction tube at a 70 °C under a N_2 atmosphere for 24 h.

The catalytic activity for this reaction is lower compared to the MOF counterpart MIL-101-NH_2-SO_3H[24a] (99%), however it is comparable to the zeolite HNaY-NS-SD[24b] (90%).

Hence, the synergistic effect of Lewis acid and basic character of the bifunctional catalyst on the reaction was established, and these cuboctahedra serve as a bifunctional nanoreactor possessing these active sites capable of interacting with the substrates, facilitating the efficient catalysis of the one-pot tandem reactions.

Conclusions

To summarize, the synthesis of bifunctional copper cuboctahedra was accomplished successfully. Through careful design of the ligand and experimental parameters, discrete cuboctahedra were formed in significant yield via self-assembly. Furthermore, these structures possess both Lewis acid and base functionalities, rendering these bifunctional catalysts suitable for catalyzing tandem reactions. The discrete metallocuboctahedra demonstrated excellent yields in catalyzing the one-pot reaction between benzaldehyde dimethyl acetal and malononitrile, with DMSO as the optimal solvent for the reaction. The catalyst could be readily separated and recovered in high yields with good recyclability, displaying negligible loss in activity over four cycles, providing further advantages. Moreover, the scope of the catalysis applications was readily expanded to other reactions as well, and the **Cu-MOP** displayed good catalytic efficacy in the one-pot deactealization-Henry reaction between benzaldehyde dimethyl acetal and nitromethane as well. Such high catalytic efficiency and versatility across tandem reactions thus introduces these nanoball architectures as new platform for catalysis.

Supporting Information

The general methods, detailed procedure for synthesis and catalytic tests, FTIR and TGA data, and additional catalysis data have been provided in the Supporting Information. The authors have cited additional references within the Supporting Information.[26–36]

Acknowledgements

The authors thank the support from the Robert A. Welch Foundation (B-0027). The authors also extend their appreciation to the Deanship of Scientific Research at Princess Nourah Bint Abdulrahman University for partially funding this work through the Visiting Researcher Program. SK acknowledges the financial support from the University Grants Commission (UGC), New Delhi, India (No. F5-80/2014(IC)). NSF's ChemMatCARS, Sector 15 at the Advanced Photon Source (APS), Argonne National Laboratory (ANL) is supported by the Divisions of Chemistry (CHE) and Materials Research (DMR), National Science Foundation, under grant number NSF/CHE-1834750. This research used resources of the Advanced Photon Source, a U.S. Department of Energy (DOE) Office of Science user facility operated for the DOE Office of Science by Argonne National Laboratory under Contract No. DE-AC02-06CH11357.

Conflict of Interests

The authors declare no conflict of interest.

Data Availability Statement

The data that support the findings of this study are available from the corresponding author upon reasonable request.

Keywords: nanoballs · metal-organic polyhedra · bifunctional · tandem catalysis · deacetalization-Knoevenagel reaction

[1] a) J.-M. Lehn, *Chem. Soc. Rev.* **2017**, *46*, 2378–2379; b) J.-M. Lehn, *Angew. Chem. Int. Ed.* **1988**, *27*, 89–112; c) J. F. Stoddart, *Nat. Chem.* **2009**, *1*, 14–15; d) F. Huang, E. V. Anslyn, *Chem. Rev.* **2015**, *115*, 6999–7000; e) W. R. Browne, B. L. Feringa, *Nat. Nanotechnol.* **2006**, *1*, 25–35; f) A. J. Savyasachi, O. Kotova, S. Shanmugaraju, S. J. Bradberry, G. M. Ó'Máille, T. Gunnlaugsson, *Chem* **2017**, *3*, 764–811; g) G. T. Williams, C. J. E. Haynes, M. Fares, C. Caltagirone, J. R. Hiscock, P. A. Gale, *Chem. Soc. Rev.* **2021**, *50*, 2737–2763.
[2] a) Y. K. Kryschenko, S. R. Seidel, A. M. Arif, P. J. Stang, *J. Am. Chem. Soc.* **2003**, *125*, 5193–5198; b) R. Chakrabarty, P. S. Mukherjee, P. J. Stang, *Chem. Rev.* **2011**, *111*, 6810–6918; c) N. B. Debata, D. Tripathy, H. S. Sahoo, *Coord. Chem. Rev.* **2019**, *387*, 273–298; d) F. M. Menger, *Proc. Nat. Acad. Sci.* **2002**, *99*, 4818–4822; e) B. Mohan, S. Shanmugaraju, in *Supramolecular Coordination Complexes* (Ed.: S. Shanmugaraju), Elsevier, **2023**, pp. 1–25; f) Y. Zhu, W. Zheng, W. Wang, H.-B. Yang, *Chem. Soc. Rev.* **2021**, *50*, 7395–7417.
[3] a) T. R. Cook, Y.-R. Zheng, P. J. Stang, *Chem. Rev.* **2013**, *113*, 734–777; b) M. J. Prakash, M. S. Lah, *Chem. Commun.* **2009**, 3326–3341; c) J. Lee, J. H. Kwak, W. Choe, *Nat. Commun.* **2017**, *8*, 14070; d) V. J. Pastore, T. R.

Cook, *Chem. Mater.* **2020**, *32*, 3680–3700; e) R. S. Forgan, *Chem. Sci.* **2020**, *11*, 4546–4562.
[4] a) J. J. I. V. Perry, J. A. Perman, M. J. Zaworotko, *Chem. Soc. Rev.* **2009**, *38*, 1400–1417; b) M. Eddaoudi, J. Kim, J. B. Wachter, H. K. Chae, M. O'Keeffe, O. M. Yaghi, *J. Am. Chem. Soc.* **2001**, *123*, 4368–4369; c) N. Ahmad, H. A. Younus, A. H. Chughtai, F. Verpoort, *Chem. Soc. Rev.* **2015**, *44*, 9–25; d) B. Moulton, J. Lu, A. Mondal, M. J. Zaworotko, *Chem. Commun.* **2001**, 863–864; e) J.-R. Li, H.-C. Zhou, *Nat. Chem.* **2010**, *2*, 893–898.
[5] a) M. B. Duriska, S. M. Neville, J. Lu, S. S. Iremonger, J. F. Boas, C. J. Kepert, S. R. Batten, *Angew. Chem. Int. Ed.* **2009**, *48*, 8919–8922, S8919/8911–S8919/8933; b) J. Park, Z. Perry, Y.-P. Chen, J. Bae, H.-C. Zhou, *ACS Appl. Mater. Interfaces* **2017**, *9*, 28064–28068; c) Y. Ke, D. J. Collins, H.-C. Zhou, *Inorg. Chem.* **2005**, *44*, 4154–4156; d) S. Furukawa, N. Horike, M. Kondo, Y. Hijikata, A. Carne-Sanchez, P. Larpent, N. Louvain, S. Diring, H. Sato, R. Matsuda, R. Kawano, S. Kitagawa, *Inorg. Chem.* **2016**, *55*, 10843–10846; e) M. D. Young, Q. Zhang, H.-C. Zhou, *Inorg. Chim. Acta* **2015**, *424*, 216–220; f) J. M. Teo, C. J. Coghlan, J. D. Evans, E. Tsivion, M. Head-Gordon, C. J. Sumby, C. J. Doonan, *Chem. Commun.* **2016**, *52*, 276–279; g) A. J. Gosselin, C. A. Rowland, K. P. Balto, G. P. A. Yap, E. D. Bloch, *Inorg. Chem.* **2018**, *57*, 11847–11850.
[6] a) A. Carne-Sanchez, J. Albalad, T. Grancha, I. Imaz, J. Juanhuix, P. Larpent, S. Furukawa, D. Maspoch, *J. Am. Chem. Soc.* **2019**, *141*, 4094–4102; b) J. Albalad, A. Carné-Sánchez, T. Grancha, L. Hernández-López, D. Maspoch, *Chem. Commun.* **2019**, *55*, 12785–12788.
[7] a) Y. Han, J.-R. Li, Y. Xie, G. Guo, *Chem. Soc. Rev.* **2014**, *43*, 5952–5981; b) H. Abourahma, A. W. Coleman, B. Moulton, B. Rather, P. Shahgaldian, M. J. Zaworotko, *Chem. Commun.* **2001**, 2380–2381; c) Y. Li, D. Zhang, F. Gai, X. Zhu, Y.-n. Guo, T. Ma, Y. Liu, Q. Huo, *Chem. Commun.* **2012**, *48*, 7946–7948; d) G. Lal, S. J. Lee, D. M. Spasyuk, G. K. H. Shimizu, *Chem. Commun.* **2018**, *54*, 1722–1725; e) J. J. I. V. Perry, V. C. Kravtsov, M. J. Zaworotko, R. W. Larsen, *Cryst. Growth Des.* **2011**, *11*, 3183–3189; f) H. Furukawa, J. Kim, K. E. Plass, O. M. Yaghi, *J. Am. Chem. Soc.* **2006**, *128*, 8398–8399.
[8] a) H. Vardhan, M. Yusubov, F. Verpoort, *Coord. Chem. Rev.* **2016**, *306*, 171–194; b) S. Lee, H. Jeong, D. Nam, M. S. Lah, W. Choe, *Chem. Soc. Rev.* **2021**, *50*, 528–555; c) A. O. Adeola, J. O. Ighalo, P. I. Kyesmen, P. N. Nomngongo, *J. CO2 Util.* **2024**, *80*, 102664; d) A. C. Ghosh, A. Legrand, R. Rajapaksha, G. A. Craig, C. Sassoye, G. Balázs, D. Farrusseng, S. Furukawa, J. Canivet, F. M. Wisser, *J. Am. Chem. Soc.* **2022**, *144*, 3626–3636; e) N. Jackson, I. R. Vazquez, Y.-P. Chen, Y.-S. Chen, W.-Y. Gao, *Chem. Commun.* **2021**, *57*, 7248–7251.
[9] a) S. M. Cohen, *Chem. Rev.* **2012**, *112*, 970–1000; b) N. Ahmad, H. A. Younus, A. H. Chughtai, K. Van Hecke, M. Danish, Z. Gaoke, F. Verpoort, *Sci. Rep.* **2017**, *7*, 832; c) D. T. Vodak, M. E. Braun, J. Kim, M. Eddaoudi, O. M. Yaghi, *Chem. Commun.* **2001**, 2534–2535; d) V. Guillerm, D. Kim, J. F. Eubank, R. Luebke, X. Liu, K. Adil, M. S. Lah, M. Eddaoudi, *Chem. Soc. Rev.* **2014**, *43*, 6141–6172; e) U. Stoeck, I. Senkovska, V. Bon, S. Krause, S. Kaskel, *Chem. Commun.* **2015**, *51*, 1046–1049; f) Y. Yan, M. Suyetin, E. Bichoutskaia, A. J. Blake, D. R. Allan, S. A. Barnett, M. Schroeder, *Chem. Sci.* **2013**, *4*, 1731–1736; g) X.-S. Wang, M. Chrzanowski, W.-Y. Gao, L. Wojtas, Y.-S. Chen, M. J. Zaworotko, S. Ma, *Chem. Sci.* **2012**, *3*, 2823–2827; h) A. Mallick, B. Garai, D. D. Díaz, R. Banerjee, *Angew. Chem. Int. Ed.* **2013**, *52*, 13755–13759; i) B. Garai, A. Mallick, A. Das, R. Mukherjee, R. Banerjee, *Chem. Eur. J.* **2017**, *23*, 7361.
[10] a) X. Liu, X. Wang, A. V. Bavykina, L. Chu, M. Shan, A. Sabetghadam, H. Miro, F. Kapteijn, J. Gascon, *ACS Appl. Mater. Interfaces* **2018**, *10*, 21381–21389; b) M. Tonigold, J. Hitzbleck, S. Bahnmüller, G. Langstein, D. Volkmer, *Dalton Trans.* **2009**, *8*, 1363–1371; c) M.-S. Kim, J. I. V. Perry, T. C. M. Julien, E. Marangon, C. Manouat, J. F. Eubank, J. P. Harmon, *J. Mater. Chem. A* **2015**, *3*, 13215–13225; d) C. R. P. Fulong, J. Liu, V. J. Pastore, H. Lin, T. R. Cook, *Dalton Trans.* **2018**, *47*, 7905–7915; e) L. Liu, N. Wang, H.-X. Liu, L. Shu, Y.-B. Xie, J.-R. Li, Q.-F. An, *J. Membr. Sci.* **2019**, *575*, 1–8; f) E. V. Perez, K. J. Balkus, J. P. Ferraris, I. H. Musselman, *J. Mem. Sci.* **2014**, *463*, 82–93.
[11] a) C. M. Vetromile, A. Lozano, S. Feola, R. W. Larsen, *Inorg. Chim. Acta* **2011**, *378*, 36–41; b) M. Tonigold, D. Volkmer, *Inorg. Chim. Acta* **2010**, *363*, 4220–4229; c) K. Omoto, N. Hosono, M. Gochomori, S. Kitagawa, *Chem. Commun.* **2018**, *54*, 7290–7293; d) R. W. Larsen, G. J. McManus, J. J. Perry IV, E. Rivera-Otero, M. J. Zaworotko, *Inorg. Chem.* **2007**, *46*, 5904–5910.
[12] a) L.-B. Sun, J.-R. Li, W. Lu, Z.-Y. Gu, Z. Luo, H.-C. Zhou, *J. Am. Chem. Soc.* **2012**, *134*, 15923–15928; b) Y.-H. Kang, X.-D. Liu, N. Yan, Y. Jiang, X.-Q. Liu, L.-B. Sun, J.-R. Li, *J. Am. Chem. Soc.* **2016**, *138*, 6099–6102; c) Y.-H. Kang, N. Yan, Z.-Y. Gao, P. Tan, Y. Jiang, X.-Q. Liu, L.-B. Sun, *J. Mater. Chem. A* **2017**, *5*, 5278–5282.
[13] a) S. Mollick, S. Mukherjee, D. Kim, Z. Qiao, A. V. Desai, R. Saha, Y. D. More, J. Jiang, M. S. Lah, S. K. Ghosh, *Angew. Chem. Int. Ed.* **2019**, *58*, 1041–1045; b) G. R. Lorzing, B. A. Trump, C. M. Brown, E. D. Bloch, *Chem. Mater.* **2017**, *29*, 8583–8587; c) E. Amayuelas, A. Fidalgo-Marijuán, B. Bazán, M.-K. Urtiaga, G. Barandika, M.-I. Arriortua, *CrystEngComm* **2016**, *18*, 1709–1712; d) M. Jung, H. Kim, K. Baek, K. Kim, *Angew. Chem. Int. Ed.* **2008**, *47*, 5755–5757; e) N. Ahmad, A. H. Chughtai, H. A. Younus, F. Verpoort, *Coord. Chem. Rev.* **2014**, *280*, 1–27.
[14] a) J. Gascon, A. Corma, F. Kapteijn, F. X. Llabrés i Xamena, *ACS Catal.* **2014**, *4*, 361–378; b) Y.-B. Huang, J. Liang, X.-S. Wang, R. Cao, *Chem. Soc. Rev.* **2017**, *46*, 126–157; c) Y. Zhang, C. Huang, L. Mi, *Dalton Trans.* **2020**, *49*, 14723–14730; d) S. Natarajan, K. Manna, *ACS Orgnic Inorganic Au* **2024**, *4*, 59–90.
[15] a) H. Furukawa, J. Kim, N. W. Ockwig, M. O'Keeffe, O. M. Yaghi, *J. Am. Chem. Soc.* **2008**, *130*, 11650–11661; b) G. J. McManus, Z. Wang, M. J. Zaworotko, *Cryst. Growth Des.* **2004**, *4*, 11–13; c) Z. Niu, S. Fang, X. Liu, J.-G. Ma, S. Ma, P. Cheng, *J. Am. Chem. Soc.* **2015**, *137*, 14873–14876; d) Z. Niu, L. Wang, S. Fang, P. C. Lan, B. Aguila, J. Perman, J.-G. Ma, P. Cheng, X. Li, S. Ma, *Chem. Sci.* **2019**, *10*, 6661–6665.
[16] R. W. Larsen, *J. Am. Chem. Soc.* **2008**, *130*, 11246–11247.
[17] X. Luo, L. Sun, J. Zhao, D.-S. Li, D. Wang, G. Li, Q. Huo, Y. Liu, *Cryst. Growth Des.* **2015**, *15*, 4901–4907.
[18] C.-L. Chen, Y. Zou, P. Qiu, Y.-H. Wen, J.-Y. Li, Z.-H. Hong, X.-M. Lin, A.-x. Xu, Y.-P. Cai, *J. Coord. Chem.* **2009**, *62*, 2480–2489.
[19] a) H. Liu, F.-G. Xi, W. Sun, N.-N. Yang, E.-Q. Gao, *Inorg. Chem.* **2016**, *55*, 5753–5755; b) L. Zhong, C. Anand, K. S. Lakhi, G. Lawrence, A. Vinu, *Sci. Rep.* **2015**, *5*, 12901; c) Z. Wang, X. Yuan, Q. a Cheng, T. Zhang, J. Luo, *New J. Chem.* **2018**, *42*, 11610–11615; d) C. Chen, N. Janoszka, C. K. Wong, C. Gramse, R. Weberskirch, A. H. Groeschel, *Angew. Chem. Int. Ed.* **2021**, *60*, 237–241; e) K. Zhou, T. Tian, C. Wang, H. Zhao, N. Gao, H. Yin, P. Wang, B. J. Ravoo, G. Li, *J. Am. Chem. Soc.* **2020**, *142*, 20605–20615; f) Z.-S. Zhao, Y. Zhang, T. Fang, Z.-B. Han, F.-S. Liang, *ACS Appl. Nano Mater.* **2020**, *3*, 6316–6320; g) M. A. Isaacs, C. M. A. Parlett, N. Robinson, L. J. Durndell, J. C. Manayil, S. K. Beaumont, S. Jiang, N. S. Hondow, A. C. Lamb, D. Jampaiah, M. L. Johns, K. Wilson, A. F. Lee, *Nat. Catal.* **2020**, *3*, 921–931; h) N. Seal, A. S. Palakkal, M. Singh, R. Goswami, R. S. Pillai, S. Neogi, *ACS Appl. Mater. Interfaces* **2021**, *13*, 28378–28389; i) H. Chen, Z. Yang, H. Peng, K. Jie, P. Li, S. Ding, W. Guo, X. Suo, J. Liu, R. Yan, W. Liu, C.-L. Do-Thanh, H. Wang, Z. Wang, L. Han, W. Yang, S. Dai, *Chem* **2021**, *7*, 3340–3358.
[20] A. C. Knipe, W. E. Watts, *Organic Reaction Mechanisms 1999: An Annual Survey Covering the Literature Dated December 1998 to November 1999*, John Wiley & Sons, Ltd, **2004**.
[21] A. Karmakar, A. Paul, G. M. D. M. Rúbio, M. M. A. Soliman, M. F. C. Guedes da Silva, A. J. L. Pombeiro, *Front. Chem.* **2019**, *7*, 699.
[22] S. Mistry, A. Sarkar, S. Natarajan, *Cryst. Growth Des.* **2019**, *19*, 747–7551.
[23] a) N. Seal, A. S. Palakkal, M. Singh, R. Goswami, R. S. Pillai, S. Neogi, *ACS Appl. Mater. Interfaces* **2021**, *13*, 28378–28389; b) A. Paul, A. Karmakar, M. da Silva, A. J. L. Pombeiro, *Catalysts* **2021**, *11*, 90; c) S. Ke, G. Chang, Z. Hu, G. Tian, D. Yang, X. Ma, K. Huang, J. Li, X. Yang, *ACS Sustainable Chem. Eng.* **2020**, *8*, 966–976; d) Y. Hu, J. Zhang, H. Huo, Z. Wang, X. Xu, Y. Yang, K. Lin, R. Fan, *Catal. Sci. Technol.* **2020**, *10*, 315–322; e) Z. Wang, X. Yuan, Q. A. Cheng, T. Zhang, J. Luo, *New J. Chem.* **2018**, *42*, 11610–11615; f) M. Zheng, Y. Wang, P. Feng, *Catalysts* **2020**, *10*, 309; g) M. Mu, X. Yan, Y. Li, L. Chen, *J. Nanopart. Res.* **2017**, *19*, 148.
[24] a) Y.-R. Lee, Y.-M. Chung, W.-S. Ahn, *RSC Adv.* **2014**, *4*, 23064–23067; b) D. Suttipat, T. Yutthalekha, W. Wannapakdee, P. Dugkhuntod, P. Wetchasat, P. Kidkhunthod, C. Wattanakit, *ChemPlusChem* **2019**, *84*, 1503–1507.
[25] Multiple datasets for the crystal were collected at USF and Argonne National Lab. Deposition Number(s) 1917306 contain(s) the supplementary crystallographic data for this paper. These data are provided free of charge by the joint Cambridge Crystallographic Data Centre and Fachinformationszentrum Karlsruhe Access Structures service.
[26] Bruker (2016). APEX3 (Version 2015.9). Bruker AXS Inc., Madison, Wisconsin, USA.
[27] Bruker (2016) SAINT V8.35A. Data Reduction Software.
[28] G. M. Sheldrick *SADABS: Program for Empirical Absorption Correction*, **1996** University of Gottingen, Germany.
[29] G. M. Sheldrick, *SHELXL-97. Program for the Refinement of Crystal*, **1997**.
[30] G. M. Sheldrick, *Acta Crystallogr.* **1990**, *A46*, 467–473.
[31] G. M. Sheldrick, *Acta Crystallogr.* **2008**, *A64*, 112–122.

[32] G. M. Sheldrick, *Acta Crystallogr.* **2010**, *D66*, 479–485.
[33] O. V. Dolomanov, L. J. Bourhis, R. J. Gildea, J. A. K. Howard, H. Puschmann, *J. Appl. Crystallogr.* **2009**, *42*, 339–341.
[34] P. Emsley, B. Lohkamp, W. G. Scott, K. Cowtan, *Acta Crystallogr.* **2010**, *D66*, 486–501.
[35] A. L. Spek, *Acta Crystallogr.* **2009**, *D65*, 148–155.
[36] R. W. W. Hooft, L. H. Straver, A. L. Spek, *J. Appl. Crystallogr.* **2008**, *41*, 96–103.
[37] Parts of this manuscript have already been published in the first author's dissertation: G. Verma, Multifunctional Metal-Organic Frameworks (MOFs) For Applications in Sustainability, University of South Florida (USF) Tampa Graduate Theses and Dissertations, **2020**.

Manuscript received: March 3, 2024
Revised manuscript received: April 2, 2024
Accepted manuscript online: April 5, 2024
Version of record online: ■■, ■■

RESEARCH ARTICLE

A bifunctional metal-organic nanoball architecture was constructed using 2,6-dimethylpyridinecarboxylic acid and copper acetate at room temperature through a straightforward synthesis approach. The resultant Cu-MOP cuboctahedra combining Lewis basic pyridine and Lewis acidic Cu(II) centers demonstrated high activity and versatility for catalyzing one-pot tandem reactions, and optimal yields were obtained utilizing DMSO as the solvent system.

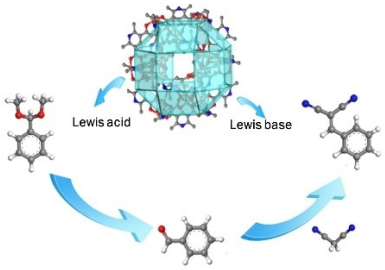

*Dr. G. Verma, Dr. S. Kumar, E. R. Slaughter, Dr. H. Vardhan, Prof. T. M. Al-shahrani, Dr. Z. Niu, Dr. W.-Y. Gao, Dr. L. Wojtas, Dr. Y.-S. Chen, Prof. S. Ma**